Yu. Senichev (FZJ, Germany), S. Andrianov (SPbU,Russia),
M. Berz (MSU, USA), S. Chekmenev (RWTH, Germany),
A. Ivanov (SPbU, Russia), E. Valetov (MSU, USA)

Investigation of lattice for deuteron EDM ring

October 12, 2015

OUTLINE

-Concept of the Frozen Spin (FS) and the Quasi-Frozen Spin (QFS) methods

-Main features of the QFS method

-FS and QFS lattices

-Spin Coherence Time vs. RF and sextupole families

-RF averaging, nonlinearities, and residual decoherence

-Tracking results

-Precursor experiments in a QFS-COSY ring

How does the QFS lattice work?

In electrostatic part

number of MDM spin oscillations relative to the momentum:

$$\nu_s^E = \left(\frac{1}{\gamma^2 - 1} - G\right)\gamma\beta^2$$

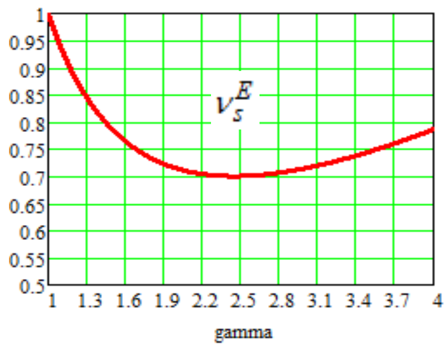

In magnetostatic part:

number of MDM spin oscillations relative to the momentum:

$$\nu_s^B = \gamma G$$

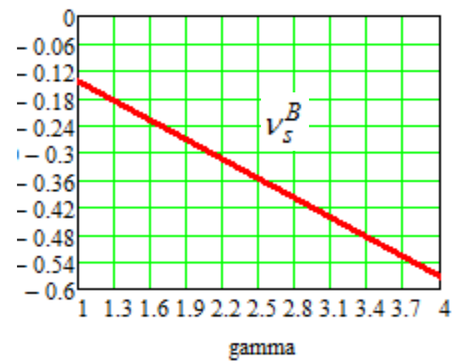

In the region 75-300 MeV, the **MDM** spin oscillates 6-7 times faster in the electric field than in the magnetic field:

In the same region of energy, the **EDM** growth is higher by the same factor 6-7 in the magnetic field than in the electric field.

Basic relations in the QFS structure between the magnetic arcs and the electrostatic arcs

Since in the electrostatic structure the spin rotates with a frequency that is $K = \frac{\nu_s^E}{\nu_s^B}$ times faster than in magnetostatic structure, we have:

$$\pi + 2\alpha = \frac{\nu_s^E}{\nu_s^B} \cdot 2\alpha \quad \text{and} \quad \Rightarrow \quad \alpha = \frac{0.5 * \pi}{(\nu_s^E / \nu_s^B) - 1}$$

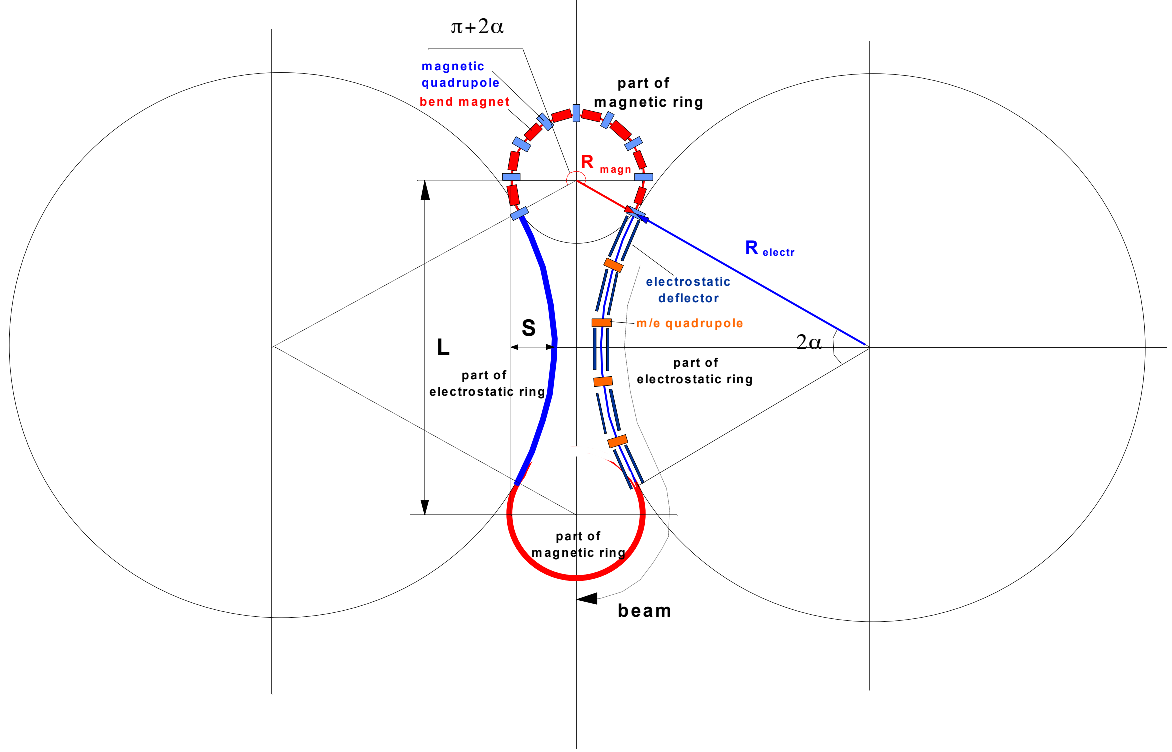

Basic relations in the QFS structure between the magnetic arcs and the static Wien filters

$$(\gamma G+1)\cdot\varphi_{SS}^{B}-\left(\gamma G+\frac{\gamma}{\gamma+1}\right)\beta^{2}\cdot\varphi_{SS}^{E}=\gamma G\cdot\varphi_{arc}^{B}$$

φ_{SS}^{B} – momentum rotation in elements due to B field

$(\gamma G+1)\cdot\varphi_{SS}^{B}$ – spin rotation in elements due to B field

$-\left(\gamma G+\frac{\gamma}{\gamma+1}\right)\beta^{2}$ – momentum rotation in elements due to E field

$-\left(\gamma G+\frac{\gamma}{\gamma+1}\right)\beta^{2}\cdot\varphi_{SS}^{E}$ – spin rotation in elements due to B field

$\gamma G\cdot\varphi_{arc}^{B}$ – spin rotation in arc due to B field

$\Rightarrow$ $L_{el}E_{el}=\frac{G}{G+1}\cdot\frac{mc^{2}}{e}\cdot\pi\beta^{2}\gamma^{3}$ and $B_{el}=-\frac{E_{el}}{c\beta}$

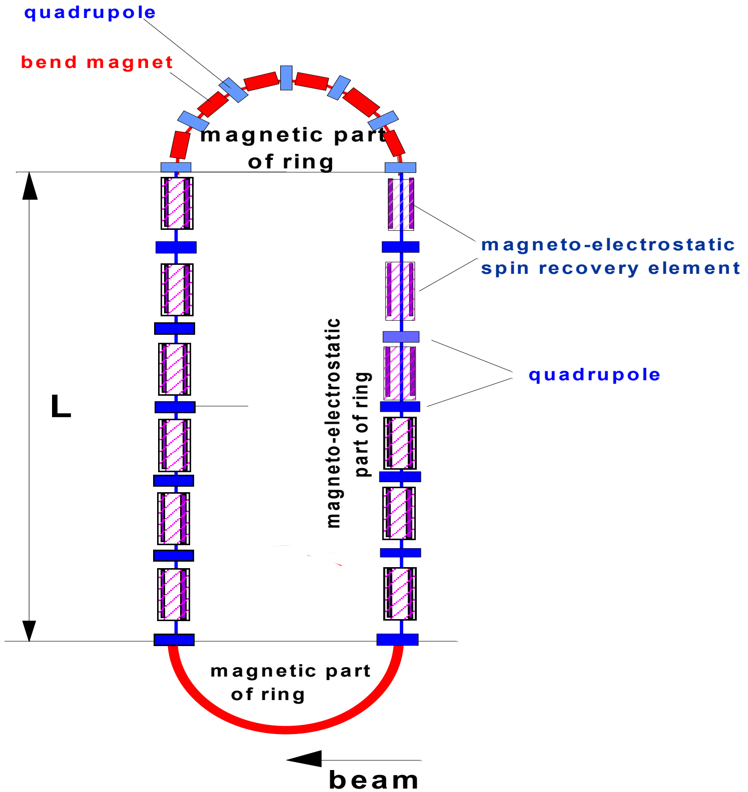

EDM growth: 3D spin-orbital simulation in MODE

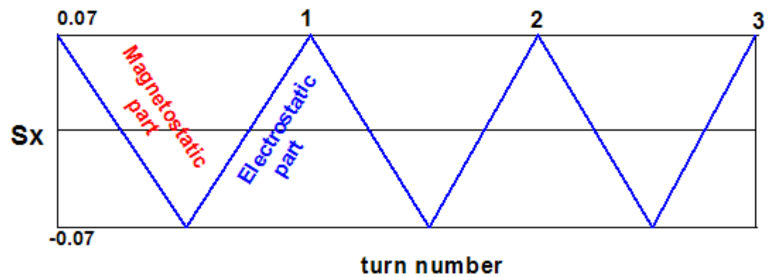

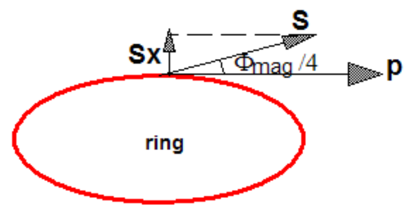

$\eta = 10^{-15}$

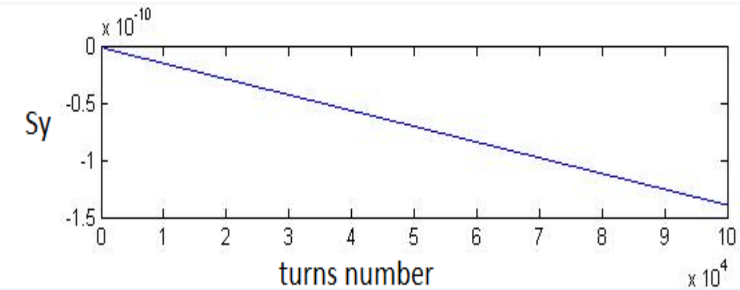

Results of the 3D spin-orbital simulation:

- Due to Sx oscillation in QFS structure, the EDM signal decreases by 1%

- In each magnet, the EDM signal grows by $-2.14133779995135 \cdot 10^{-16}$ and in each deflector by $3.20268895179507 \cdot 10^{-17}$

- Total EDM signal grows by $-1.39074513140842 \cdot 10^{-15}$ per turn

- In order to get total EDM signal $\sim 10^{-6}$ we have to keep the beam in the ring during $N_{turn} \sim 10^{9}$ or **~800 sec**

FS Lattice with BNL elements

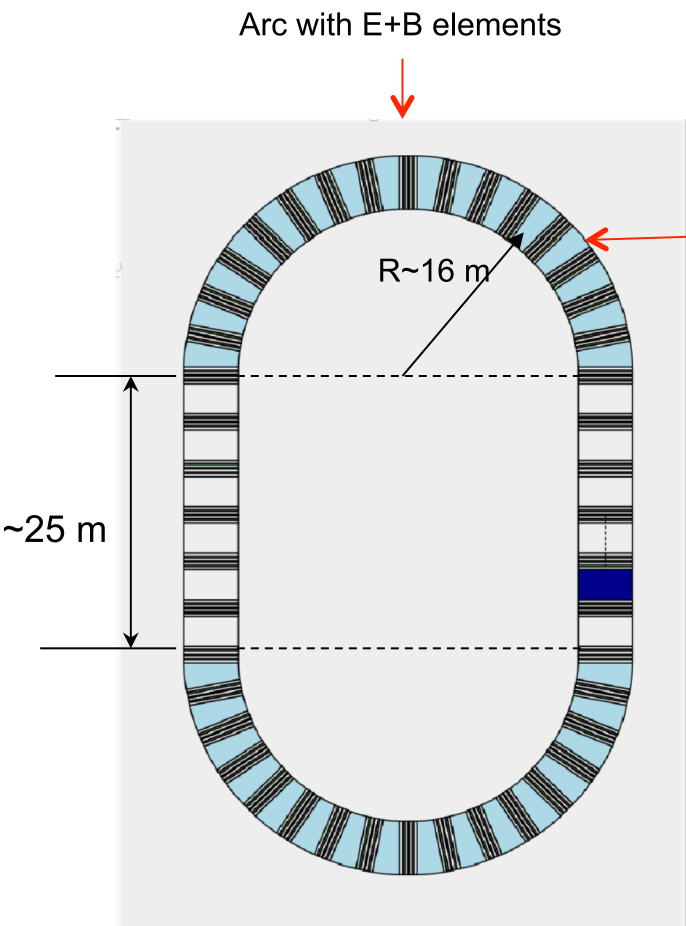

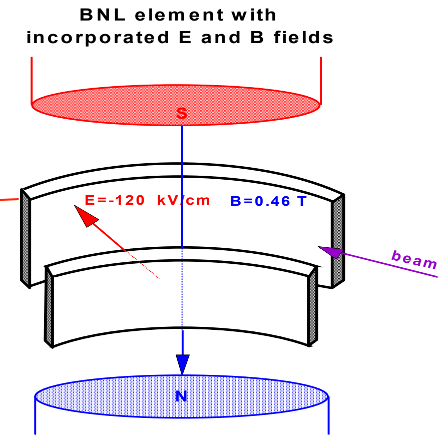

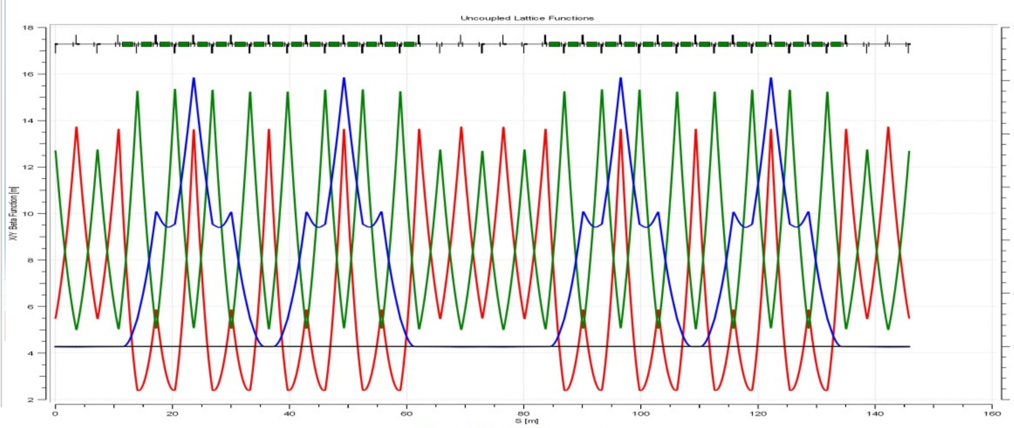

QFS Lattice with the electrostatic arcs

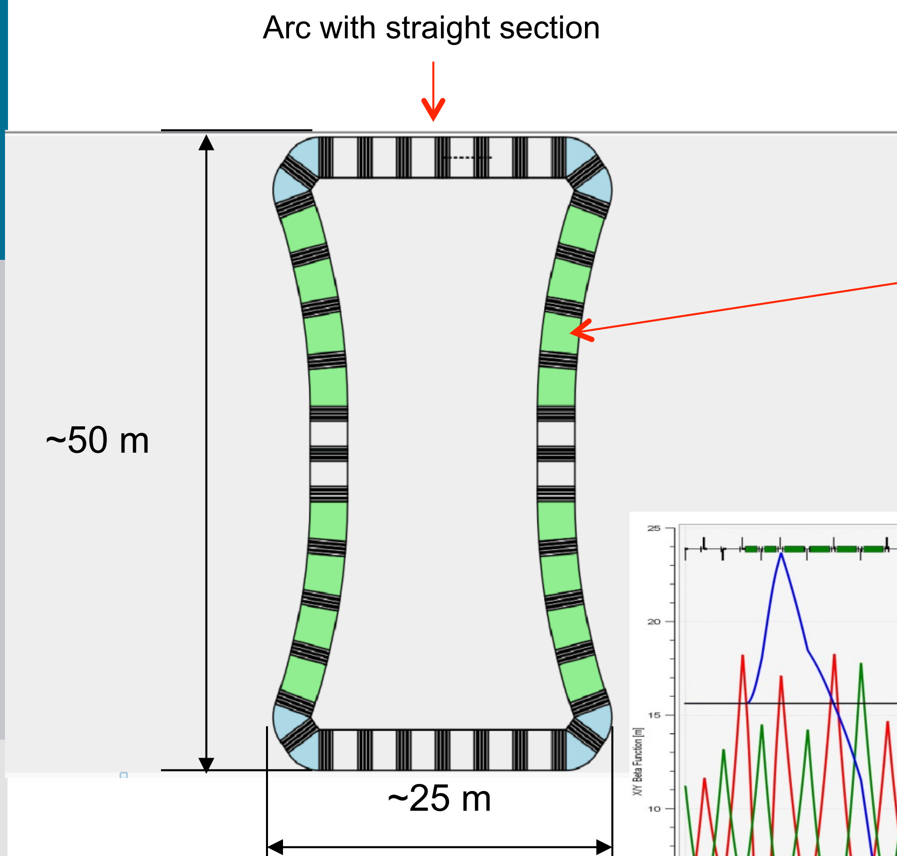

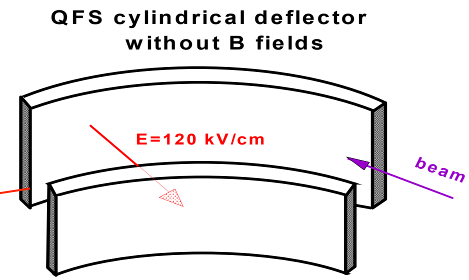

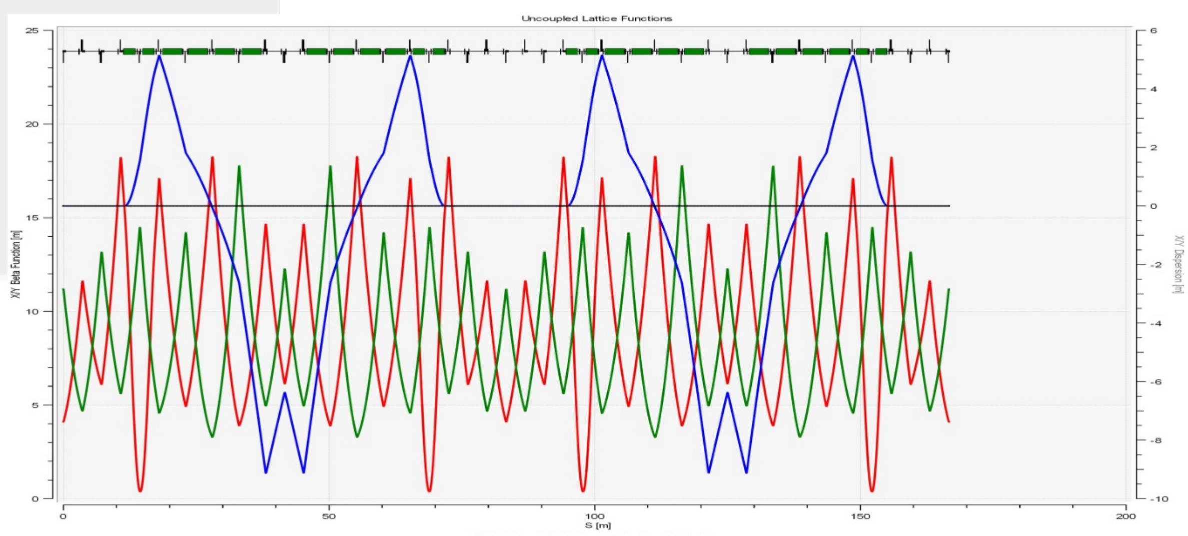

QFS lattice with static Wien filters

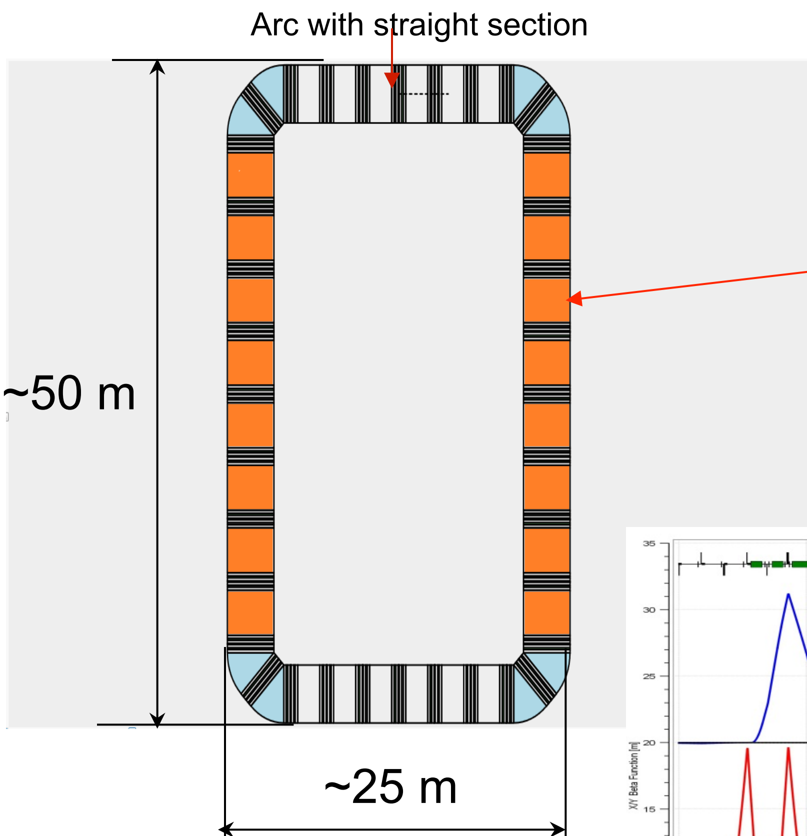

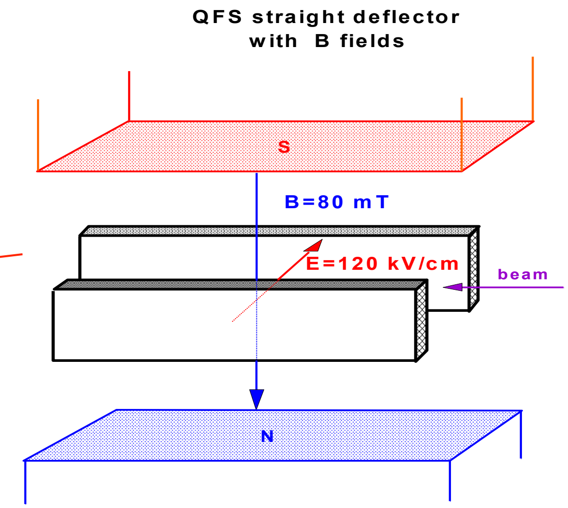

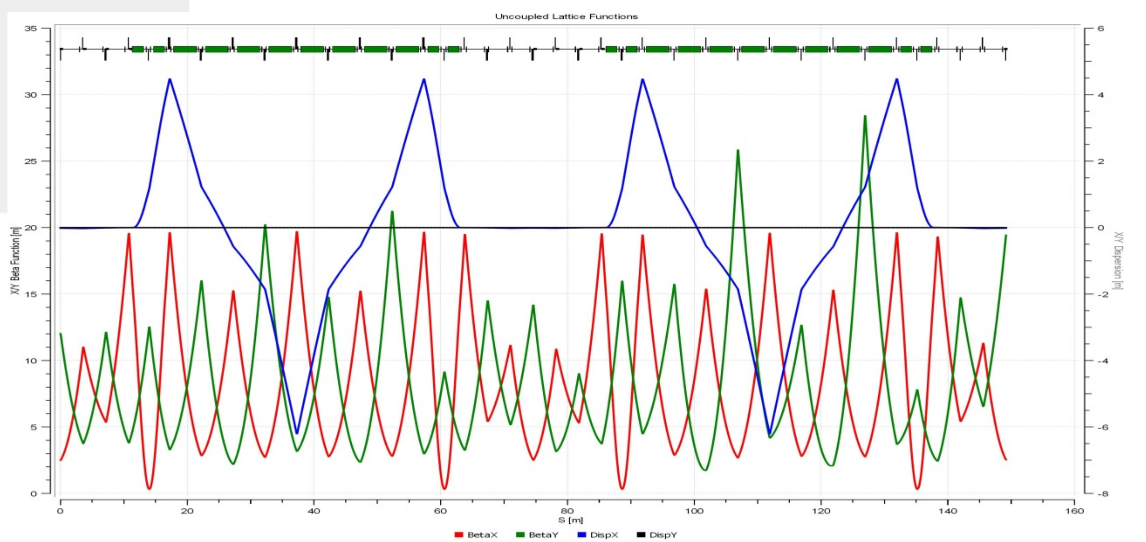

Cylindrical deflector

$$r'' - \frac{1}{r} + \frac{1}{R_{eq}^2} r = 0$$

Plate deflector

$$\frac{d^2x}{ds^2} = -\frac{2eU_0}{mv_\vartheta^2 d}$$

$$\frac{d^2y}{ds^2} = 0$$

Parameters of the 3 lattices at W_d =270 MeV

Energy	FS lattice with BNL elements	QFS lattice with electrostatic arcs	QFS lattice with static Wien filters
Number FODO cells	22 cells	18 cells	18 cells
Number of quadrupole magnets, effective length, gradient (T/m)	44; 0.2 m; 4÷6 T/m	36; 0.2 m; 4÷5 T/m	36; 0.2 m; 5÷6 T/m
Number of bend magnets, field (T), length (m), radius of curvature		8; 1.5 T; 1.8 m; 2.3 m	8; 1.5 T; 1.8 m; 2.3 m
Number of electrostatic deflectors, field, length, radius of curvature	32 def; E=120 kV/cm; B=0.46 T; L=1.8m; R=9.2 m	16def; E=120 kV/cm; L= 3.6 m; R=42 m	16def;E=120 kV/cm; B=0.08T; L=3.6m; R=∞
Circumference, m	145 m	149 m	149 m
Momentum compaction factor	0.03	0.1	0.07
Maximum dispersion, m	3.0 m	-6÷5	-6÷4.5
Number of straight sections with D≠0 and D=0 , length	**2x20.4 m; (D=0)**	2x7.5 m;(D≠0) **2x23 m; (D=0)**	**2x23.2 m; (D=0)**
Maximum beta function value in X and Y planes	$ß_x$ 10 m; $ß_y$ changes in range 10÷500 m	$ß_x$ 20 m; $ß_y$ changes in range 20÷500 m	$ß_x$ =18 m; $ß_y$ can be changed in range 20÷500 m
Tune, X and Y	ν_x= 4.8; ν_y= 2.8÷0.4	ν_x= 4.56; ν_y= 3.53÷0.2	ν_x= 4.9; ν_y= 3.9÷0.1
Number of sextupoles, effective length, gradient	N=26; two families; L=0.15 m; S_x= 24 T/m^2; S_y=43 T/m^2	N=27; six families; L=0.15 m; S= 4÷5 T/m^2	N=27; six families; L=0.15 m; S= 3÷10 T/m^2

Dynamic aperture for the 3 lattices

Arc with BNL elements

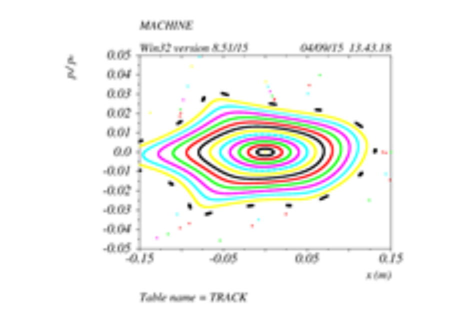

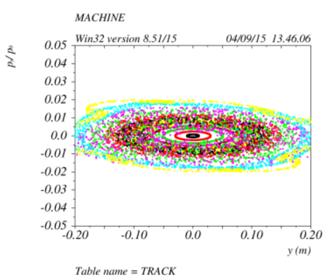

B arc + E arc

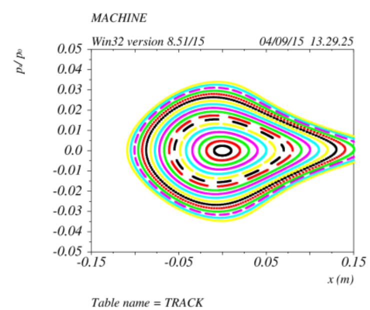

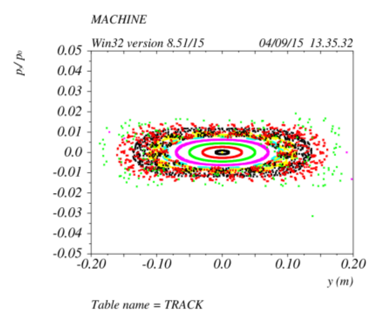

B arc + static Wien filter

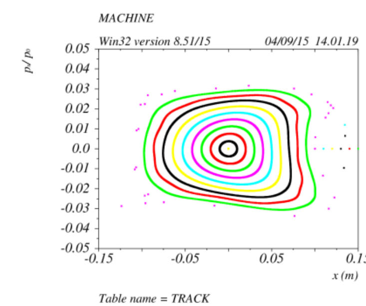

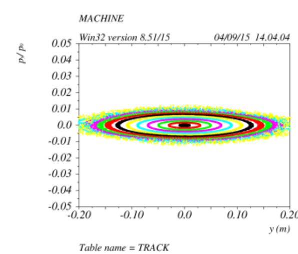

Spin Coherence Time vs. RF field and sextupole families

The spin tune spread in the magnetic field relative to the momentum:

$$\nu_s^B = \frac{\Omega_S^B - \Omega_p^B}{\Omega_p^B} = -\gamma|G| \longrightarrow \Delta\nu_s^B = -\Delta\gamma\cdot|G|$$

The spin tune spread in the electric field relative to the momentum:

$$\nu_s^E = \frac{\Omega_S^E - \Omega_p^E}{\Omega_p^E} = \frac{1}{\gamma}(1-|G|) + \gamma|G| \longrightarrow \Delta\nu_s^E = \Delta\gamma\cdot|G| - \frac{1}{\gamma_0^2}(1-|G|)\Delta\gamma + \frac{1}{\gamma_0^3}(1-|G|)\Delta\gamma^2 - \ldots$$

nonlinear term of spin tune

Longitudinal motion:

x and y orbit lengthening

$$\frac{d\varphi}{dt} = -\omega_{rf}\left[\left(\alpha_0 - \frac{1}{\gamma^2}\right)\cdot\delta + \left(\alpha_1 - \frac{\alpha_0}{\gamma^2} + \frac{1}{\gamma^4}\right)\cdot\delta^2 + \left(\frac{\Delta L}{L}\right)_\beta\right]$$

$$\frac{d\delta}{dt} = \frac{eV_{rf}\omega_{rf}}{2\pi h\beta^2 E}\sin\varphi$$

nonlinear term of energy oscillation

Spin Coherence Time vs. RF field and sextupole families

Energy oscillation:

$$\Delta\gamma = \gamma_0\beta_0^2\left\{\delta_0\cos 2\pi\nu_z n + \left(\frac{\alpha_1}{\eta}-\frac{1}{\gamma_0^2}\right)\delta_0^2\cos 4\pi\nu_z n + \left(\frac{\alpha_1}{\eta}-\frac{1}{\gamma_0^2}\right)\delta_0^2 + \frac{1}{\eta}\left(\frac{\Delta L}{L}\right)_\beta\right\}$$

Substituting $\Delta\gamma$ in the spin tune spread in the electric

$$\Delta\nu_s^E = \Delta\gamma\cdot|G| - \frac{1}{\gamma_0^2}\left(1-|G|\right)\Delta\gamma + \frac{1}{\gamma_0^3}\left(1-|G|\right)\Delta\gamma^2 - \ldots \rightarrow \left\langle\Delta\nu_s^E\right\rangle_{Nturns} \approx \left[\underbrace{\frac{\alpha_1}{\gamma_0\eta}\delta_0^2}_{\text{Nonlinear Z motion}} + \underbrace{\frac{\beta_0^2}{\eta\gamma_0}\left(\frac{\Delta L}{L}\right)_\beta}_{\text{Betatron motion}} + \underbrace{\frac{\beta_0^4}{\gamma_0}\delta_0^2}_{\text{Nonlinearity of spin tune}}\right]\cdot Nturns$$

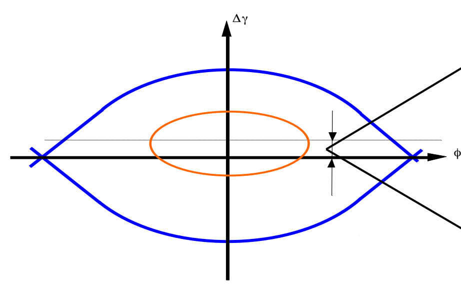

$$\left(\frac{\Delta L}{L}\right)_\beta = \frac{\pi}{2L}\left[\frac{\nu_x}{\beta_x}x^2 + \frac{\nu_y}{\beta_y}y^2\right]$$

and the magnetic fields: $\Delta\nu_s^B = -\Delta\gamma\cdot|G|$

$$\rightarrow \left\langle\Delta\nu_s^B\right\rangle_{turns} \approx \left[\underbrace{\frac{\alpha_1}{\gamma_0\eta}\delta_0^2}_{\text{Nonlinear Z motion}} + \underbrace{\frac{\beta_0^2}{\eta\gamma_0}\left(\frac{\Delta L}{L}\right)_\beta}_{\text{Betatron motion}}\right]\cdot Nturns$$

Sextupole families

To minimize the spin decoherence due to final emittances and energy spread in the bunch, we use 6 sextupole families:

$$-\frac{\varepsilon_x}{2L}\sum_i S_i l_{si} D_{xi} \beta_{xi} = \frac{\pi}{2L}\varepsilon_x \nu_x$$

$$\frac{\varepsilon_y}{2L}\sum_i S_i l_{si} D_{xi} \beta_{yi} = \frac{\pi}{2L}\varepsilon_y \nu_y$$

$$-\frac{\delta^2}{L}\sum_i S_i l_{si} D_{xi}^3 = \alpha_1 \delta^2$$

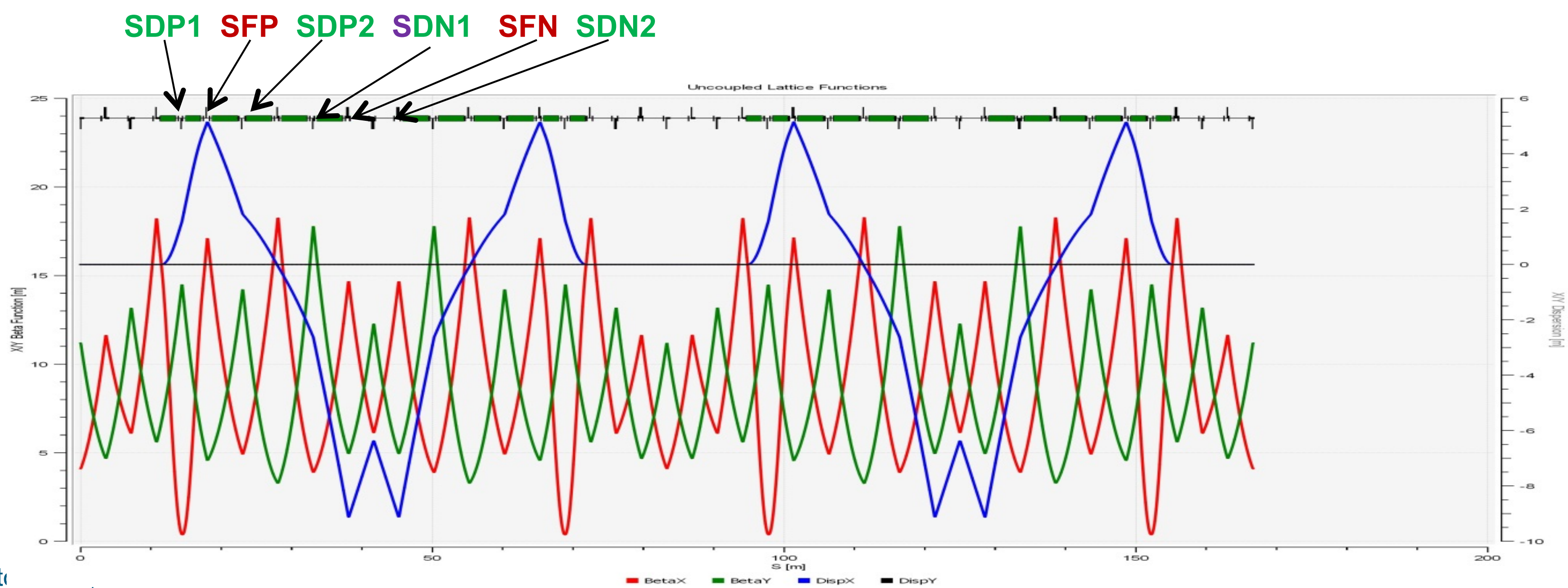

Spin Coherence Time vs. RF field and sextupole families

We have minimized spin decoherence using all families of sextupoles

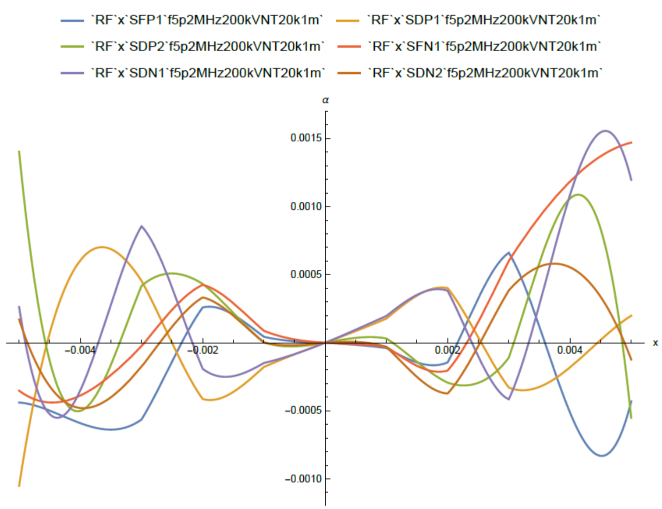

x is a spacial amplitude of the particle

α is the angle offset of the particle's spin, relative to the reference particle

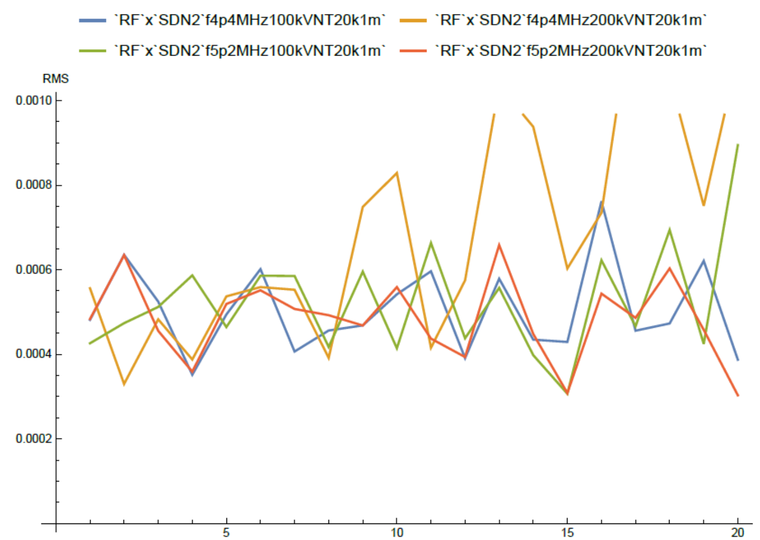

N is the tracking step number

RMS is the root mean square of α at points of grid that spans x-interval

Dynamic aperture vs. sextupole families

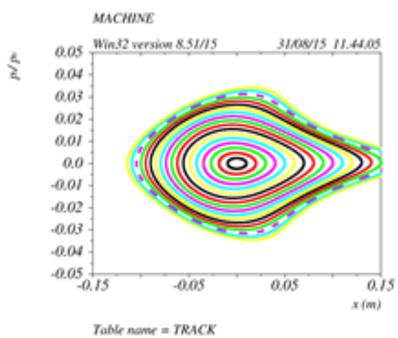

X: SDP1 and SFP1

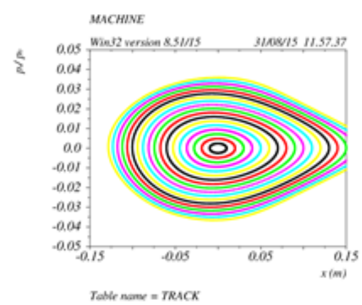

X: SDP1 and SFN1

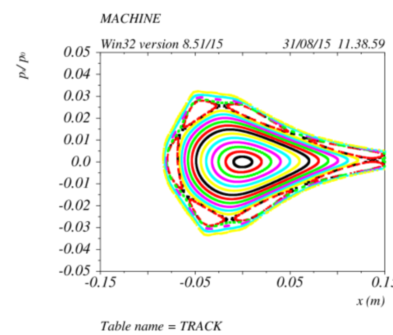

X: SDP2 and SFP1

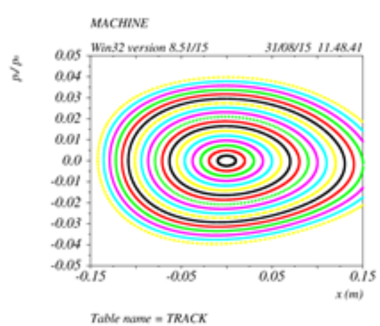

X: SDN2 and SFN1

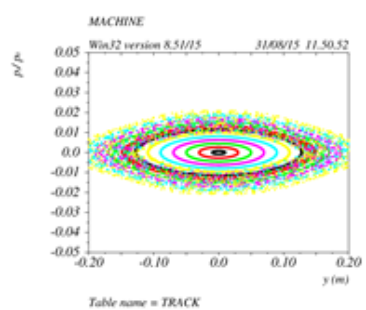

Y: SDN2 and SFN1

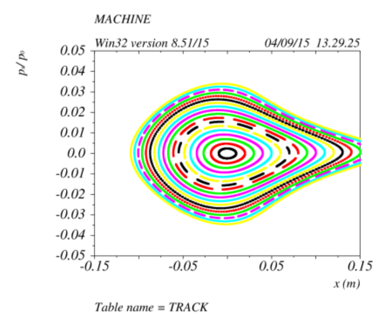

X: all families at optimum chromaticity correction

Residual decoherence

1. In transverse plane: uncompensated higher-than-sextupole order field, e.g. in the cylindrical deflector

$$E_R = \frac{2U_0}{\ln\frac{R_2}{R_1}} \cdot \frac{1}{r}$$

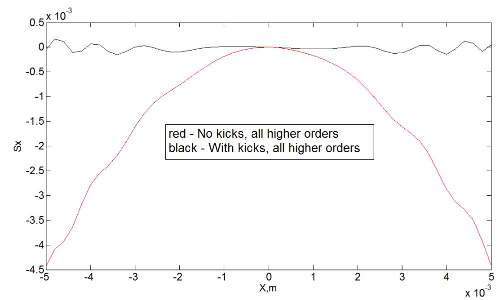

2. RF field modulation

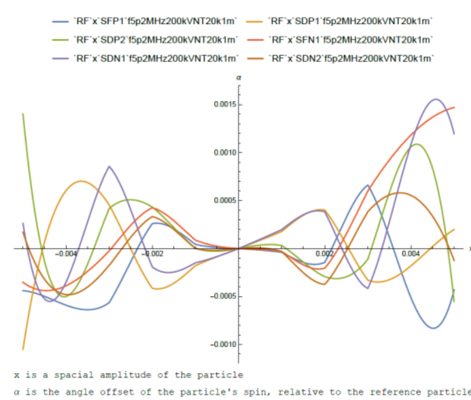

Precursor experiments in a QFS-COSY ring

Since for precursor experiment we do not need large statistics, we can start working QFS at the 75 MeV. It is then sufficient to use only 4 “E+B” straight elements, which is four times less than at 270 MeV. The total length is 2x7 m. Further, they can be used for a full scale experiment at 270 MeV. To reduce the cost of rework, permanent magnet technology can be used with the field 120-100 mT. The condition for compensation of spin rotation is fulfilled using the E field (working regime 120 kV/cm).

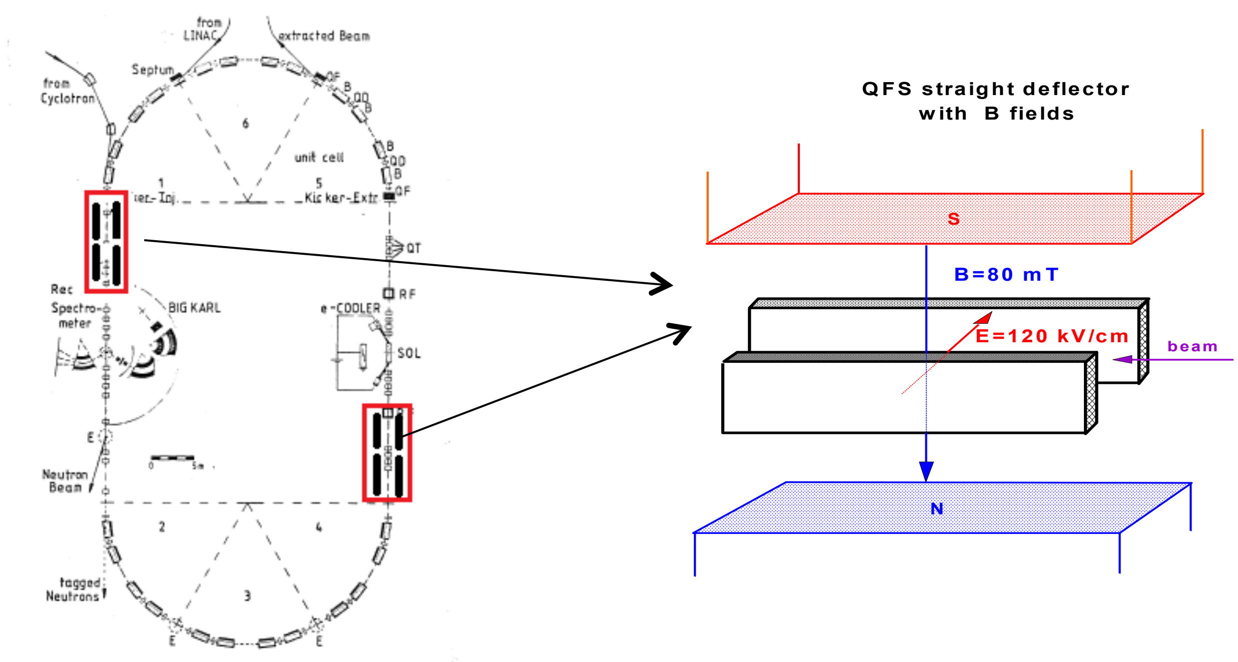

Conclusion

- The proposed QFS method does not restrict to one energy value and provides an EDM signal using simpler elements.
- The structures based on separated E and B fields and static Wien filters are much easier and cheaper than those required by the FS method.
- Reduction of the number of elements for the precursor experiment would proportionally reduce the cost (to 1-2 M€ maximum) and make it possible to work with the QFS in the COSY ring in the shortest timeframe.
- The lattice meets all requirements for EDM search.